PHILOSOPHICAL TRANSACTIONS OF THE ROYAL SOCIETY A MATHEMATICAL, PHYSICAL & ENGINEERING SCIENCES

The Initiation and Propagation of Travelling Waves on Membrane Interfaces in the Belousov-Zhabotinskii Reaction

J. A. Leach, J. H. Merkin and S. K. Scott

Phil. Trans. R. Soc. Lond. A 1993 **345**, 229-258
doi: 10.1098/rsta.1993.0129

The initiation and propagation of travelling waves on membrane interfaces in the Belousov–Zhabotinskii reaction

By J. A. Leach[1], J. H. Merkin[1] and S. K. Scott[2]

[1]*Department of Applied Mathematics, and* [2]*School of Chemistry, University of Leeds, Leeds LS2 9JT, U.K.*

Contents

Travelling reaction–diffusion waves are considered in a simplified model of the Belousov–Zhabotinskii reaction, described mathematically by the two-variable Oregonator. A one-dimensional problem consisting of two regions is considered. Region I (effectively the boundary at $x' = 0$) acts as a reservoir with a fixed concentration of the autocatalytic species (hypobromous acid), and provides constant input of this species into region II. Region II (the reaction zone $0 < x' < \infty$) allows diffusion of the autocatalyst while the catalytic species Ce^{IV} is assumed immobilized on a supporting matrix.

The form of the ensuing travelling wavefront and the behaviour in the region behind the front as it propagates into the region of increasing x', is considered. By examining the large time behaviour it is shown that the propagating front travels with its minimum possible wave speed. Both single travelling waves and periodic wave trains are observed.

Phil. Trans. R. Soc. Lond. A (1993) **345**, 229–258
Printed in Great Britain

1. Introduction

Travelling waves of chemical or other activity are common features of spatially distributed systems. In many of these systems, the medium through which the reaction wave propagates is said to be 'excitable'. Excitable media are characterized by a stable state that is relatively insensitive to small perturbations but when subjected to a stimulus above some threshold responds through a single large excursion. In the Belousov–Zhabotinskii (BZ) system for example, this can be revealed by a transient colour change in the reaction mixture. In unstirred BZ systems, the travelling waves can be followed by this transient red–blue colour change. If the system is subjected to some periodic stimulus, periodic wave trains of excitation and recovery develop (Tyson & Keener 1988; Murray 1989).

In this paper, we consider a reaction–diffusion problem based on a simplified model for the Belousov–Zhabotinskii chemistry. The kinetic scheme we use to represent the BZ reaction is based on a reduced form of the Oregonator (Field & Noyes 1973; Field & Troy 1979; Tyson 1979; Tyson & Fife 1980; Crowley & Field 1984). This has five reaction steps involving only the three intermediates hypobromous acid ($HBrO_2$), the bromide ion (Br^-), and the oxidized form of the metal–ion catalyst (Ce^{IV}) and is given by

$$\mathrm{A}+\mathrm{Y}\rightarrow\mathrm{X}+\mathrm{P}, \qquad \text{rate} = k_3 AY, \tag{1a}$$

$$\mathrm{X}+\mathrm{Y}\rightarrow 2\mathrm{P}, \qquad \text{rate} = k_2 XY, \tag{1b}$$

$$\mathrm{A}+\mathrm{X}\rightarrow 2\mathrm{X}+2\mathrm{Z}, \qquad \text{rate} = k_5 AX, \tag{1c}$$

$$2\mathrm{X}\rightarrow \mathrm{A}+\mathrm{P}, \qquad \text{rate} = k_4 X^2, \tag{1d}$$

$$\mathrm{B}+\mathrm{Z}\rightarrow \tfrac{1}{2}f\mathrm{Y}, \qquad \text{rate} = k_0 BZ, \tag{1e}$$

where the k_i are the rate constants and where we assume that the concentrations of species A and B are constant. Here X, Y and Z denote the concentrations of $HBrO_2$ (the autocatalyst), Br^- and Ce^{IV} respectively. P denotes the concentration of HOBr; this species is a product and plays no active part in the overall reaction.

Further, we assume (as in Tyson (1979) and Tyson & Fife (1980)) that the concentration of the bromide ion (Br^-) adjusts rapidly to the instantaneous composition of the reacting mixture. This then implies, from (1), that

$$Y = \tfrac{1}{2}fk_0 BZ/(k_3 A + k_2 X) \tag{2}$$

and the mechanism can be described fully in terms of the concentrations of the species represented by X and Z.

The experimental configuration of particular interest here is that reported in a sequence of recent papers by Showalter and co-workers (Maselko *et al.* 1989; Maselko & Showalter 1989, 1991; Winston *et al.* 1991) namely one in which the metal–ion catalyst is immobilized on some supporting matrix. The catalyst-loaded matrix may take the form of ion-exchange beads, with wave activity confined to the surface of a single bead or occurring across a surface formed by many beads in contact, or an ion-exchange membrane. The matrix is immersed in a solution of the remaining BZ reagents at suitable concentrations. In the case of the (thin) membrane, waves may develop on either side but these do not propagate completely independently of each other. Instead there is a coupling through the membrane. Because of the high net negative charge within the matrix, anionic species such as BrO_3^- or Br^- do not penetrate to any significant extent, so coupling presumably arises by diffusion of neutral species such as the autocatalyst $HBrO_2$. The strength of the coupling (i.e. the

effective diffusion coefficient) varies with, and hence can be controlled by, the loading of the membrane with the metal–ion: the higher the degree of loading the lower the effective diffusion coefficient. By varying the experimental constraints, various 'patterns', many without obvious precedent in 'homogeneous' reaction–diffusion situations, have been observed, including apparent phase-locking between waves of different inherent frequencies creating a regular 'mosaic' across both surfaces. Spatiotemporal structures deriving from coupled waves on membrane surfaces may have wider significance, perhaps in biological systems, or provide new ways of coupling different reactions or reactors. At present, the theoretical understanding of the possible processes is also not well developed for coupled waves.

To develop a theoretical model, we first seek a robust relevant model that produces a periodic wavetrain on one surface, preferably without a periodic stimulus at its centre. Here we concentrate on an essentially one-dimensional problem without coupling, with two regions I (effectively the boundary at $x' = 0$) and II (the reaction zone $0 < x' < \infty$). Region I acts as a reservoir with a fixed concentration of the autocatalytic species X. This provides input to region II. In region II, the autocatalyst can diffuse but species Z is immobile. We find that the imposition of a constant concentration of X at $x' = 0$ can cause the formation of a suitable periodic wavetrain if the parameters of the model correspond to an oscillatory or an excitable state of the corresponding well-stirred system. In this paper, we examine the basic form of the wavefront, its velocity and the solution 'left behind' as it propagates into the region of increasing x'.

2. Governing equations and dimensionless variables

The equations governing the diffusion and reaction of species X and Z on the membrane are, on using the kinetic scheme derived from (1) and (2), for planar geometry,

$$\frac{\partial X}{\partial t'} = D_x \frac{\partial^2 X}{\partial x'^2} + \left(\frac{k_3 A - k_2 X}{k_3 A + k_2 X}\right) \tfrac{1}{2} f k_0 B Z + k_5 A X - 2k_4 X^2, \tag{3a}$$

$$\partial Z/\partial t' = 2k_5 A X - k_0 B Z, \tag{3b}$$

where x' and t' are the space and time variables respectively.

Equations (3) also requires some initial and boundary conditions. We assume that the concentrations of the bromide ion and the oxidized form of the metal catalyst are initially zero everywhere within the membrane, and that at time $t' = 0$, the edge of the membrane, $(x' = 0)$ is placed in contact with the reservoir of the autocatalyst $HBrO_2$, which is then kept at a constant concentration X_0 throughout. This leads to the initial and boundary conditions

$$\left.\begin{aligned} X &= X_0 \quad \text{on} \quad x' = 0, \\ X &\to 0 \quad \text{as} \quad x' \to \infty, \end{aligned}\right\} \quad t' \geqslant 0, \tag{4a}$$

and

$$X = Z = 0 \quad \text{at} \quad t' = 0 \quad (0 < x' < \infty). \tag{4b}$$

Equations (3) are made non-dimensional by writing

$$u = 2k_4 X/k_5 A, \quad v = \frac{k_5 k_0}{(k_4 A)^2} BZ, \tag{5a}$$

$$t = k_0 B t', \quad x = (k_5 A/D_x)^{\frac{1}{2}} x'. \tag{5b}$$

PHILOSOPHICAL TRANSACTIONS OF THE ROYAL SOCIETY A MATHEMATICAL, PHYSICAL & ENGINEERING SCIENCES

On using (5), equations (3) and initial and boundary conditions (4) become

$$\varepsilon\frac{\partial u}{\partial t}=\frac{\partial^2 u}{\partial x^2}+u(1-u)+fv\frac{(q-u)}{(q+u)}, \tag{6a}$$

$$\partial v/\partial t = u-v, \tag{6b}$$

subject to

$$\left.\begin{aligned} u &= u_0 && \text{on} \quad x=0,\\ u &\to 0, \quad v\to 0 && \text{as} \quad x\to\infty, \end{aligned}\right\} \quad t\geqslant 0, \tag{7a}$$

$$u=v=0 \quad \text{in} \quad 0<x<\infty, \quad t=0. \tag{7b}$$

The dimensionless parameters, q, ε and u_0 are defined by

$$q=2k_3k_4/k_2k_5, \quad \varepsilon=k_0B/k_5A, \quad u_0=2k_4X_0/k_5A. \tag{8}$$

These, together with the stoichiometric factor f, specify the system. The parameter q is usually taken to be small (typically $q=0.0008$) due to the magnitude of the rate constant k_2. The parameter ε is considered to be within the range $0<\varepsilon\leqslant 1$. The value of the parameter u_0 the non-dimensionalized concentration of the autocatalyst on the boundary can take all values but here is taken to be of order unity. Throughout we shall be using the stoichiometric factor f as the bifurcation parameter.

As a necessary first step in attempting to understand the behaviour of the reaction–diffusion system given by equations (6, 7), as detailed description of the corresponding 'well-stirred' or kinetic system is required. This we now review.

3. The kinetic system

The basic kinetics for the two-variable Oregonator model are given by equations (6) with the diffusion term put to zero. This spatially homogeneous system has two, physically acceptable, stationary states (u_s, v_s) given by

$$u_s=v_s=0, \tag{9a}$$

$$u_s=v_s=\tfrac{1}{2}\{1-(f+q)+\sqrt{[(f+q-1)^2+4q(f+1)]}\}. \tag{9b}$$

It is important to note that the parameter ε does not occur in either stationary state, also stationary state (9a) corresponds to the initial conditions for our reaction–diffusion system.

It is straightforward to show that stationary state (9a) is a saddle point for all values of the parameters, whereas stationary state (9b) admits Hopf bifurcations, the conditions for which are given parametrically by

$$\varepsilon=1-2u_s\left(1+\frac{fq}{(q+u_s)^2}\right) \tag{10}$$

(the associated limit cycle produced by the Hopf bifurcation being unstable).

Suppose that the parameter q is held fixed, then a curve of Hopf bifurcation points can be plotted in the ε, f parameter plane. However, for these to exist in the positive quadrant $\varepsilon, f>0$, the parameter q must satisfy the relation

$$q<q_* \quad (q_*\approx 0.075). \tag{11}$$

Figure 1a shows the ε, f parameter plane for a value of the parameter $q=0.0008$. The

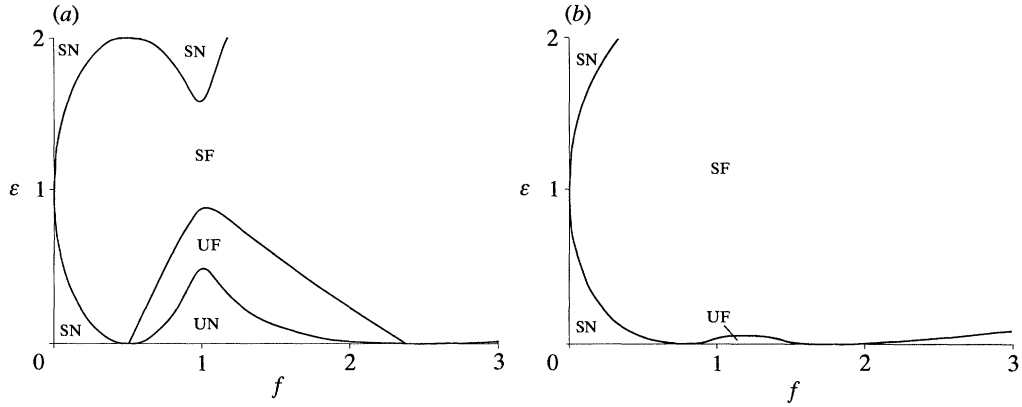

Figure 1. ε, f parameter plane, depicting the regions within which stationary state (9*b*) is a stable node (SN), stable focus (SF), unstable node (UN) or a unstable focus (UF). (*a*) $q = 0.0008$, (*b*) $q = 0.007$.

regions in which the stationary state (9*b*) is a stable node (SN), stable focus (SF), unstable focus (UF) and unstable node (UN) are also shown. The curve separating the regions of stable and unstable focal behaviour corresponds to the curve of Hopf bifurcations. This curve separates the regions in which stationary state (9*b*) is stable and unstable. As q approaches q_* the region of oscillatory behaviour (the region in which stationary state (9*b*) is unstable) in the positive quadrant shrinks until at $q = q_*$ this region of oscillations disappears altogether, leaving stationary state (9*b*) stable for all positive values of the parameters ε and f. This is illustrated in figure 1*b* by a plot of the ε, f parameter plane for $q = 0.07$.

In general, the parameter q will be small; here we shall be taking it fixed at the value $q = 0.0008$ for all the results presented below. We complete this section by considering the form of the stationary state (9*b*) and Hopf bifurcation curve (10) in (ε, f) parameter space for $q \ll 1$.

An examination of (9*b*) for $q \ll 1$ shows that there are three separate cases to be considered, namely $f < 1$, $f > 1$ and $|1-f|$ small, of $O(q^{\frac{1}{2}})$. For the first two cases, we find after a little calculation, that

$$u_s = (1-f) + (2f/(1-f))\,q + \ldots, \quad \text{for} \quad f < 1, \tag{12a}$$

$$u_s = ((f+1)/(f-1))\,q + \ldots, \quad \text{for} \quad f > 1, \tag{12b}$$

A consideration of the higher order terms in expansions (12) shows that these breakdown when $|1-f|$ is of $O(q^{\frac{1}{2}})$. To examine this case further we put $f = 1 + Aq^{\frac{1}{2}}$, where A is of $O(1)$ in this region. This leads to

$$u_s = \tfrac{1}{2}[\sqrt{(A^2+8)} - A]\,q^{\frac{1}{2}} + \frac{1}{2}\left[\frac{3A}{\sqrt{(A^2+8)}} - 1\right]q + \ldots \tag{13}$$

for $|1-f| \ll 1$. Note that (13) agrees with (12*a*) as $A \to -\infty$ and with (12*b*) as $A \to \infty$.

Expressions (12*a*, *b*) and (13) gives a complete description of the steady state u_s for small q. Starting from small values of f, u_s falls rapidly as f is increased and becomes small as $f \to 1$. In the neighbourhood of $f = 1$, u_s is small, $O(q^{\frac{1}{2}})$, as given by (13). As f is increased still further, u_s decreases even more to $O(q)$, as given by (12*b*). This is illustrated in figure 2 where we give a plot of u_s against f for $q = 0.0008$.

Expressions (12) and (13) can be used in (10) to obtain expressions for the Hopf

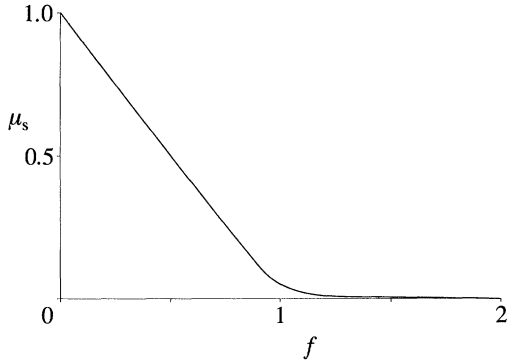

Figure 2. A graph of u_s against f for $q = 0.0008$.

bifurcation curve for $q \ll 1$. We find, again after a little calculation, that these are given by

$$\varepsilon = (2f-1) - \frac{6f}{(1-f)}q + \ldots, \quad \text{for} \quad f < 1, \tag{14a}$$

$$\varepsilon = \frac{2f+1-f^2}{2f} + \ldots, \quad \text{for} \quad f > 1, \tag{14b}$$

$$\varepsilon = 1 - [\sqrt{(A^2+8)} - A]\left[1 + \frac{4}{(\sqrt{(A^2+8)}-A)^2}\right]q^{\frac{1}{2}} + \ldots \tag{14c}$$

for $|1-f|$ small, with again $f = 1 + Aq^{\frac{1}{2}}$. Note that (14c) agrees with (14a) as $A \to -\infty$ and with (14b) as $A \to \infty$. The expansions (14) compare very well with the almost triangular Hopf bifurcation curve depicted in figure 1a, with the maximum range of Hopf bifurcation (on $\varepsilon = 0$) given by

$$\tfrac{1}{2} + 3q + \ldots < f < 1 + \sqrt{2} + O(q). \tag{15}$$

Finally we note that the maximum on the Hopf bifurcation curve occurs when $f \approx 1$, and taking $f = 1$ (i.e. $A = 0$) we obtain

$$u_s = \sqrt{2}q^{\frac{1}{2}} - \tfrac{1}{2}q + \ldots, \tag{16a}$$

$$\varepsilon = 1 - 3\sqrt{2}q^{\frac{1}{2}} + \tfrac{5}{2}q + \ldots. \tag{16b}$$

Equation (16b) shows that $\varepsilon = 0$ when $q = 2/25$, giving an approximate value for $q_* = 0.08$, which compares well with the numerically determined value given in (11).

We are now in a position to discuss the reaction–diffusion initial-value problem given by equations (6) and (7).

4. The initial-value problem

(a) *Small time solution*

The initial spread of u into the membrane ($x > 0$) is by diffusion. This suggests introducing the variable $\eta = x/t^{\frac{1}{2}}$, and with $u = u(\eta, t)$, $v = v(\eta, t)$, equations (6) become

$$\varepsilon\left(t\frac{\partial u}{\partial t} - \frac{\eta}{2}\frac{\partial u}{\partial \eta}\right) = \frac{\partial^2 u}{\partial \eta^2} + tF(u,v), \tag{17a}$$

$$t\frac{\partial v}{\partial t} - \frac{\eta}{2}\frac{\partial v}{\partial \eta} = t(u-v), \tag{17b}$$

PHILOSOPHICAL TRANSACTIONS OF THE ROYAL SOCIETY A MATHEMATICAL, PHYSICAL & ENGINEERING SCIENCES

subject to

$$\left.\begin{aligned} u &= u_0 && \text{on} && \eta = 0, \\ u &\to 0, \quad v \to 0 && as && \eta \to \infty, \end{aligned}\right\} \; t \geqslant 0. \tag{18}$$

Here $F(u, v)$ represents the reaction terms on the right-hand side of equation (6*a*). The form of equations (17) suggests looking for a solution by expanding

$$u(\eta, t) = U_0(\eta) + tU_1(\eta) + \ldots, \tag{19a}$$

$$v(\eta, t) = V_0(\eta) + tV_1(\eta) + \ldots . \tag{19b}$$

On substituting expansions (19) into equations (17) and equating terms in like powers of t, we obtain equations for the U_i and V_i ($i = 0, 1, 2, \ldots$) which can be solved in turn so as to satisfy boundary conditions (18). We find that

$$U_0(\eta) = \frac{u_0 \sqrt{\varepsilon}}{\sqrt{\pi}} \int_\eta^\infty \mathrm{e}^{-\varepsilon s^2/4} \, \mathrm{d}s, \tag{20a}$$

$$V_0(\eta) = 0, \tag{20b}$$

and, at $O(t)$, that

$$U_1(\eta) = \frac{u_0}{\sqrt{\pi}} \left(\frac{1}{\sqrt{\varepsilon}} \int_\eta^\infty \mathrm{e}^{-\varepsilon s^2/4} \, \mathrm{d}s - \mathrm{e}^{-\varepsilon \eta^2/4} \, U(\tfrac{3}{2}; \tfrac{1}{2}; \tfrac{1}{4}\varepsilon\eta^2) \right), \tag{21a}$$

$$V_1(\eta) = \frac{u_0 \sqrt{\varepsilon}}{\sqrt{\pi}} \left\{ \left(\frac{\varepsilon\eta^2}{2} + 1 \right) \int_\eta^\infty \mathrm{e}^{-\varepsilon s^2/4} \, \mathrm{d}s + \eta \, \mathrm{e}^{-\varepsilon\eta^2/4} \right\} \tag{21b}$$

(where (21*a*) is expressed in terms of a confluent hypergeometric function (Slater 1960)).

We can use this expansion to calculate the initial influx of reactant X into the membrane. This is given, in dimensionless terms, by $-(\partial u/\partial x)_{x=0}$, and using (20) and (21) we find that

$$-\left(\frac{\partial u}{\partial x} \right)_{x=0} = \frac{u_0 \sqrt{\varepsilon}}{\sqrt{\pi}} \left(1 + \left(\frac{1}{\varepsilon} - 2 \right) t + \ldots \right) \tag{22}$$

(22) shows that the effect of the reaction is first felt at $O(t)$ in this expansion.

(*b*) *Bounds on the solution*

Consider first the case $q \leqslant 1$. It is straightforward to show that the set

$$\mathscr{S} = \{(u, v) : 0 \leqslant u \leqslant 1 + u_0, \quad 0 \leqslant v \leqslant 1 + u_0\} \tag{23}$$

satisfies the conditions of theorem 5.17 of Britton (1986) and hence is an invariant rectangle for the system. Consequently, since our solution starts in this rectangle at $t = 0$, it remains bounded (and in $\mathscr{S}$) for $t > 0$. A further consequence of this is (by theorem 5.18 in Britton (1986), that the initial-boundary value problem, given by (6) and (7), has a unique global solution.

Furthermore, if we restrict u_0 so that $u_0 \leqslant 1$, we can show that the set

$$\mathscr{S}_1 = \{(u, v) : 0 \leqslant u \leqslant 1, \quad 0 \leqslant v \leqslant 1\} \tag{24}$$

is also an invariant rectangle for our system. Hence, in this case, we have the bound,

$$0 \leqslant u(x, t) \leqslant 1, \quad 0 \leqslant v(x, t) \leqslant 1 \tag{25}$$

for all $t \geqslant 0$, $0 \leqslant x < \infty$.

Also, we can show that for the, perhaps unrealistic, case when $q > 1$ and $u_0 \leqslant 1$ the corresponding invariant rectangle is

$$\mathscr{S}_2 = \{(u, v) : 0 \leqslant u \leqslant q, \quad 0 \leqslant v \leqslant q\} \tag{26}$$

Finally in this section, we note that equation (6*b*) can be integrated, subject to initial condition (7*a*), to give $v(x, t)$ in terms of $u(x, t)$ as

$$v(x, t) = \mathrm{e}^{-t} \int_0^t u(x, s)\, \mathrm{e}^s \, \mathrm{d}s \tag{27a}$$

(27*a*) shows that on $x = 0$

$$v(0, t) = u_0(1 - \mathrm{e}^{-t}) \tag{27b}$$

and hence $v(0, t) \to u_0$ as $t \to \infty$. Also, with $0 \leqslant u(x, t) \leqslant 1$, the bound, $0 \leqslant v(x, t) \leqslant 1$, implied in $\mathscr{S}_1$ is recovered.

We now go on to consider the solution for u_0 small. This will show that the initial configuration of the system, $u = v = 0$ is unstable to small perturbations, growing exponentially quickly away from, initially small, values of u and v. Then, invoking the boundedness (24) or (26) and uniqueness of the solution we can conjecture that, for large time, reaction–diffusion travelling waves will be set up.

(*c*) *Solution for small* u_0

To obtain a solution of equations (6) valid for $u_0 \ll 1$ we set,

$$u = u_0 U, \quad v = u_0 V. \tag{28}$$

Then, on assuming that $q \gg u_0$, we obtain the linearized system

$$\varepsilon \frac{\partial U}{\partial t} = \frac{\partial^2 U}{\partial x^2} + U + fV, \tag{29a}$$

$$\partial V / \partial t = U - V, \tag{29b}$$

at leading order, subject to the initial and boundary conditions, derived from (6),

$$\left.\begin{aligned} U &= 1 && \text{on} \quad x = 0, \\ U \to 0, \quad V &\to 0, && \text{as} \quad x \to \infty, \end{aligned}\right\} \quad t \geqslant 0, \tag{30a}$$

$$U = V = 0 \quad \text{at} \quad t = 0, \quad 0 < x < \infty. \tag{30b}$$

The initial-value problem given by (29) and (30) can be solved using Laplace transforms. We find that $U(x, t)$ is then calculated from the integral

$$U(x, t) = \frac{1}{2\pi \mathrm{i}} \int_{p_0 - \mathrm{i}\infty}^{p_0 + \mathrm{i}\infty} \frac{1}{p} \exp\left(- \left[\frac{(p - p_0)(p + p_1)}{p + 1} \right]^{\frac{1}{2}} x \sqrt{\varepsilon} \right) \mathrm{e}^{pt} \, \mathrm{d}p, \tag{31a}$$

where the constants p_0 and p_1 are defined in terms of ε and f by

$$p_0 = \frac{\sqrt{[(1+\varepsilon)^2 + 4\varepsilon f]} + (1 - \varepsilon)}{2\varepsilon}, \quad p_1 = \frac{\sqrt{[(1+\varepsilon)^2 + 4\varepsilon f]} - (1 - \varepsilon)}{2\varepsilon}$$

with it being straightforward to show that $p_1 > 1$ and $p_0 > 1/\varepsilon$. For the function $((p - p_0)(p + p_1)/(p + 1))^{\frac{1}{2}}$ in integral (31*a*) branch cuts are taken from $p = p_0$ to $p = -1$ and from $p = -p_1$ to $p \to -\infty$ along the real axis, with the argument taken

to be zero for $p > p_0$ on the positive real axis. The contour integral in (31*a*) can be transformed into an integral on the positive real axis to give

$$U(x,t) = \frac{\mathrm{e}^{p_0 t}}{\pi}\int_0^\infty \frac{\mathrm{e}^{-R\cos\theta}}{p_0^2+r^2}\left(p_0\cos\left(rt-R\sin\theta\right)+r\sin\left(rt-R\sin\theta\right)\right)\mathrm{d}r, \tag{31b}$$

where
$$R = \frac{r^{\frac{1}{2}}x\sqrt{\varepsilon}}{\sqrt{[(p_0+1)^2+r^2]}}\left[\left((p_0+p_1)(p_0+1)+r^2\right)^2+(p_1-1)^2r^2\right]^{\frac{1}{4}}$$

and
$$\theta = \tfrac{1}{4}\pi - \arctan\left[\frac{(p_1-1)\,r}{(p_0+1)(p_0+p_1)+r^2}\right],$$

with the principal value taken for the inverse tangent.

The main interest in (31) is the behaviour of $U(x,t)$ for t large. This can be done most efficiently directly from the Laplace transform (31*a*) in which we first put $S = (p-p_0)t$ to get

$$U(x,t) = \frac{\mathrm{e}^{p_0 t}}{2\pi\mathrm{i}}t^{-1}\int_{-\mathrm{i}\infty}^{\mathrm{i}\infty}\frac{1}{((S/t)+p_0)}\exp\left(-\frac{S^{\frac{1}{2}}((S/t)+p_0+p_1)^{\frac{1}{2}}x\sqrt{\varepsilon}}{((S/t)+p_0+1)^{\frac{1}{2}}t^{\frac{1}{2}}}\right)\mathrm{e}^S\,\mathrm{d}S. \tag{32a}$$

Now, putting $\eta = x/t^{\frac{1}{2}}$ and letting $t\to\infty$ in (32*a*) we obtain

$$U(x,t) \sim \frac{\mathrm{e}^{p_0 t}}{2\pi\mathrm{i}}\frac{t^{-1}}{p_0}\exp\int_{-\mathrm{i}\infty}^{\mathrm{i}\infty}\left(-S^{\frac{1}{2}}\left(\frac{p_0+p_1}{p_0+1}\right)^{\frac{1}{2}}\sqrt{\varepsilon}\eta\right)\mathrm{e}^S\,\mathrm{d}S \tag{32b}$$

for η of $O(1)$. Then, by a standard Laplace transform (Watson 1981),

$$U(x,t) \sim \frac{\sqrt{\varepsilon}}{2\sqrt{\pi p_0}}\left(\frac{p_0+p_1}{p_0+1}\right)^{\frac{1}{2}}\frac{\eta}{t}\mathrm{e}^{p_0 t}\exp\left(-\frac{(p_0+p_1)\,\varepsilon\eta^2}{4(p_0+1)}\right) \tag{32c}$$

as $t\to\infty$ with η of $O(1)$.

We note that (32*c*) remains uniform for η large but becomes non-uniform as $\eta\to 0$, in particular when η is of $O(t\,\mathrm{e}^{-p_0 t})$, i.e. when x is of $O(t^{\frac{3}{2}}\mathrm{e}^{-p_0 t})$. Further, we note that when x is of $O(1)$, U is of $O(\mathrm{e}^{p_0 t})$, growing exponentially quickly, while when $x \gg t \gg 1$, U remains exponentially small.

(*d*) *Numerical solutions*

The initial-value problem given by equations (6) and (7) was solved numerically using essentially the same method described in detail in Merkin & Needham (1989) and used for the numerical integration of a range of related reaction–diffusion problems by Merkin *et al.* (1989), Merkin & Needham (1990, 1991) and Gray *et al.* (1990).

The numerical scheme is a modified Crank–Nicolson method, in which the derivatives in the t-direction are replaced by forward differences and all of the terms averaged over the step form t to $t+\Delta t$. This results in two coupled ordinary differential equations in x which are then differenced using central differences. The resulting sets of nonlinear algebraic equations are solved by Newton–Raphson iteration, a process which was found to converge very quickly.

The integration from t to $t+\Delta t$ was performed in first one and then two steps and the difference between the two solutions monitored. If this was less than some preset tolerance (usually set at 5×10^{-4}) the integration was deemed to have achieved the required accuracy. Otherwise, the time step was halved and the process repeated. This procedure was found necessary to maintain accuracy in the reaction–diffusion

front as it propagated forwards. The actual time steps used varied and depended critically on the propagation speed of the front, the faster the speed, the smaller the time step needed. We found that using the above criterion, Δt ranged from 0.02 to 0.0025.

The position of the reaction–diffusion front was taken as the point where $\partial u/\partial x$ took its maximum value. This was used to calculate the wave speed (using central differences in time). The position of the wave front for the case when a wave train was set up (as described below), as well as the positions of the successive maxima in this wave train, were also calculated from the positions of the maxima in u and v. The speed of propagation of all these maxima could also then be calculated. We are considering a spatially continuous excitable medium, in which the interaction of neighbouring elements through diffusion can produce travelling waves of excitation. Diffusion allows the wave front to propagate forwards through the medium by exciting the medium ahead of the front and hence allowing further reaction. The propagating wave front converts the perturbed unstable stationary state (9*a*) to the stable stationary state (9*b*) as it travels through the medium or, if this stationary state is also unstable, a succession of waves travel through the medium (wave train).

In the numerical results presented below, the parameter q was fixed at a value of 0.0008, which is sufficiently small to allow both single travelling waves and wave trains to be observed. The parameter u_0 was also fixed at a value of $u_0 = 1.0$, this value being chosen arbitrarily, since it has already been seen, from the small u_0 solution, that there is no minimum value of u_0 below which travelling waves are not initiated. The size of the parameter u_0 controls the time scale over which travelling waves are first seen (Merkin & Needham 1989, 1991). Since the growth rate is linear in u for small u was can deduce that this timescale will depend only weakly on u_0, and can estimate it to be of $O(\log 1/u_0)$ for u_0 small.

Travelling waves were observed to exist for all values of the parameters ε and f chosen. Single travelling waves and wave trains were initiated in the heterogeneous medium for values of the parameters ε and f for which the well-stirred system is non-oscillatory and oscillatory respectively.

We present wave profiles for two values of the parameter ε, namely 0.3 and 0.05. The former of these values was chosen to exemplify the features of the wave profiles, which the latter, although more physically realistic, requires much larger amounts of computational effort to generate the wave profiles due to the much increased wave speed. Values of the parameter f were chosen to give the required types of wave profile for the values of ε above. First consider single travelling waves for the physically realistic value of the parameter ε, namely 0.05. Figure 3*a*, *b* (for $f = 0.005$ and $f = 0.4$ respectively) illustrates the development of single travelling reaction–diffusion fronts, converting the unstable stationary state (9*a*) to the stable stationary state (9*b*), here $u_s = v_s = 0.9950$ (for $f = 0.005$) and $u_s = v_s = 0.6011$ (for $f = 0.4$). Here we see an initial sharp increase in u (the non-dimensional concentration of hypobromous acid) followed, for $f = 0.4$, by a more gradual decrease to its stationary state value. This decrease occurs due to the adjustment of the bromide ion concentration via equation (2). Essentially hypobromous acid is consumed as it acts as a reducing agent for the bromate to produce bromide ions. This reduction continues until stationary state concentrations are obtained. In both cases the increase in v (the dimensionless concentration of Ce^{IV}) is monotone and in the case of $f = 0.005$ requires a larger spatial distance to reach the stable state at the rear of the wave.

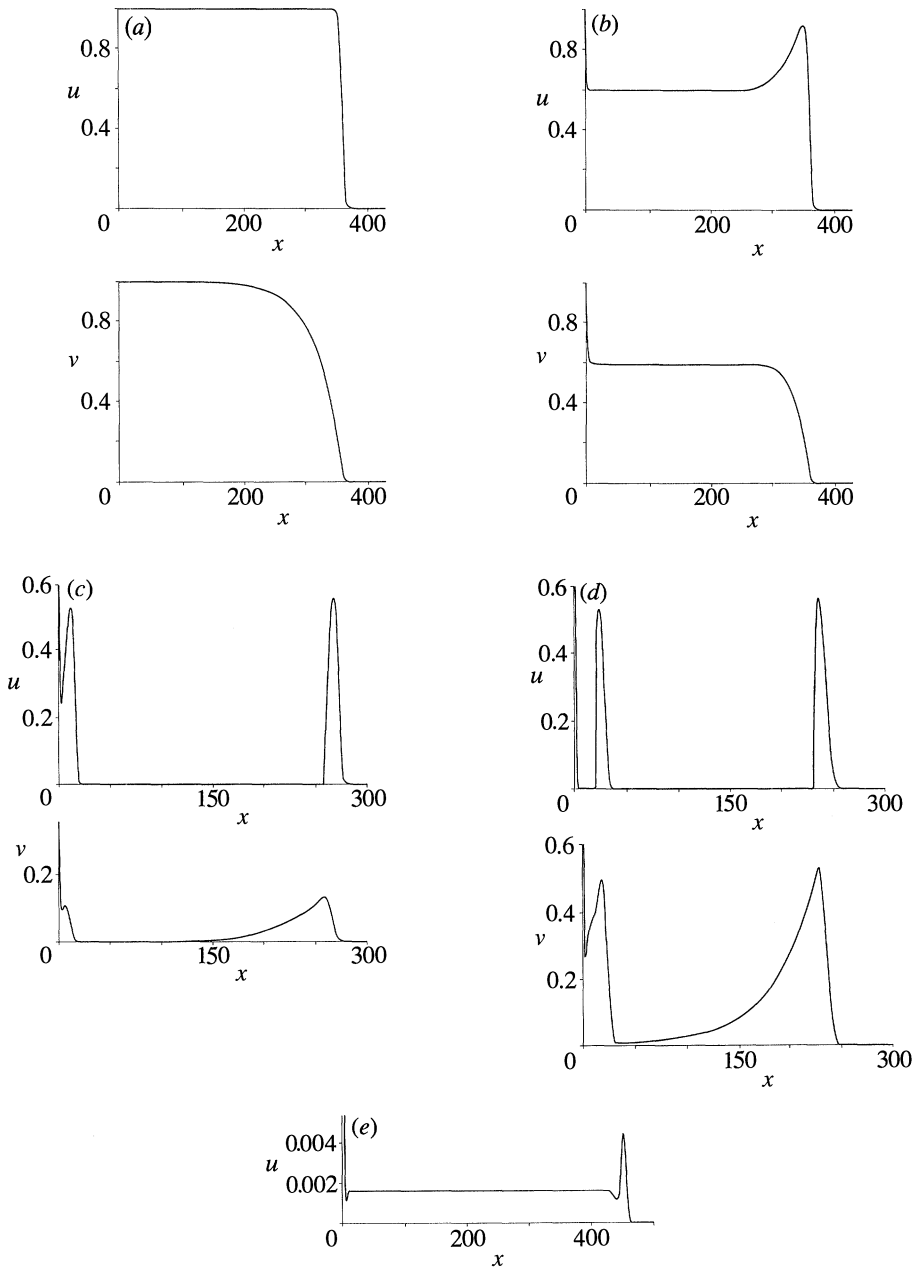

Figure 3. Concentration profiles of u and v, showing the travelling wave (*a*) $f = 0.005$, $u_0 = 1$, (*b*) $f = 0.4$, $u_0 = 1$, (*c*) $f = 3.0$, $u_0 = 1$, (*d*) $f = 3.0$, $u_0 = 10$, with $\varepsilon = 0.05$ and $q = 0.0008$, and (*e*) $f = 3.0$, $u_0 = 10$, $\varepsilon = 0.3$ and $q = 0.0008$.

The cases shown in figure 3*a*, *b* are for values of f less than the lower Hopf bifurcation point (see figure 1*a*). The situation for values of f above the upper Hopf bifurcation point is more complicated. This is illustrated in figure 3*c*, *d* for $f = 3.0$. In figure 3*c* (for $u_0 = 1.0$ and $\varepsilon = 0.05$) we can see that there is a propagating reaction–diffusion front, pulse-like in u and ramp-like in v. This has clearly detached itself from the behaviour near the boundary and is moving forwards with constant

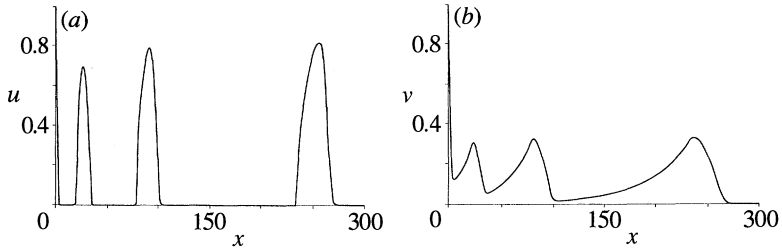

Figure 4. Concentration profiles of u and v, showing a wavetrain of travelling waves, for $\varepsilon = 0.05$, $f = 1.0$ and $q = 0.0008$.

velocity. However, unlike the previous cases, the values of u and v at the rear of this wave are not the steady state values $u = v = u_s$ (here $u_s = 0.0016$), but now u remains at the constant value $u = q$, while v decreases slowly. There is also a region near the boundary where it appears that another pulse in u is about to be detached. We examined this point a little more by taking $u_0 = 10.0$ (with the other parameters at their previous values). The results are shown in figure 3*d*, where we can see that a second pulse in u has now become completely detached from the boundary leaving behind another region in which $u = q$. We conjecture that this process repeats itself indefinitely. However, we are unable to confirm this within the computing resources available to us, though computations done in a finite region using essentially the same equations discussed here do show a regular train of propagating pulses in u being detached from the boundary regions (Leach 1991).

This firing of regular pulses in u from the boundary when the stationary state u_s is stable requires small values of ε. For $\varepsilon = 0.3$ (with the results shown in figure 3*e*) the situation is essentially the same as for values of f less than the lower Hopf bifurcation point, with u and v having their stable stationary state values $u = v = u_s$ at the rear of the propagating reaction–diffusion front.

Next consider the wave trains: these can be observed at values of the parameters ε and f for which the stationary state (9*b*) is unstable. We first consider the physically realistic value of the parameter ε, namely $\varepsilon = 0.05$. Figure 4 illustrates a wave front propagating away from the boundary leaving behind an incipient wave train. Note the very gradual ramp-like structure at the back of the wave in the profile for v, with a sharp, pulse-like structure for u.

The computational time required to produce a fully developed wave train consisting of a wave front followed by several waves behind it for $\varepsilon = 0.05$ was found to be unacceptably large. To treat this phenomenon in more detail with the expenditure of a more reasonable amount of computational effort, a larger value of the parameter ε must be chosen. To do this we took $\varepsilon = 0.3$ and figure 5*a–c* displays waves trains for $f = 0.75$, 1.0 and 1.5 respectively. The wave profiles can be considered to consist of three regions. First, there is the wave front in which u and v are perturbed from their initially unreacted state. This is followed by the wave train, in which waves are successively formed near the boundary and then adjust their amplitude and velocity so as to develop a regular wave train behind the reaction–diffusion front. Note that the waves just behind this front are travelling with the same velocity as the front. For $f = 0.75$ and 1.0 (figure 5*a*, *b*) the reaction–diffusion front has a very similar appearance to the waves in the wave train. However, this is not the case for $f = 1.5$ (figure 5*c*) where the front has a much larger amplitude than the waves in the wave train. The third region consists of a local

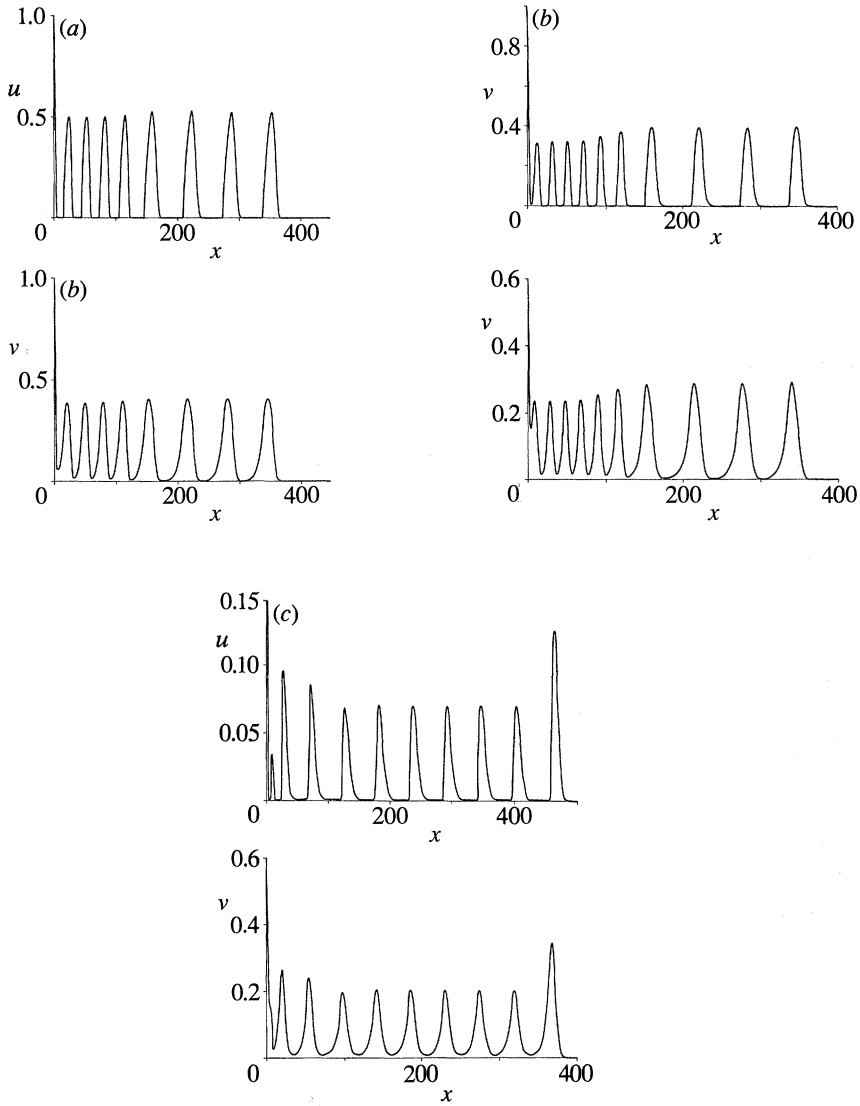

Figure 5. Concentration profiles of u and v, showing a wavetrain of travelling waves for $\varepsilon = 0.3$, $q = 0.0008$. (*a*) $f = 0.75$, (*b*) $f = 1.0$, (*c*) $f = 1.5$.

region in which u diffuses into the medium from the boundary. Within this region waves are fired, after a wave has been initiated the medium here is, at first, refractory to the propagation of another wave of excitation. Gradually the system recovers its excitability, ready for another wave to be fired, with this process then being successively repeated.

There are two features of these wave trains that are worth noting. First, the fully established wave profiles have the same appearance as the oscillatory response curves for the well-stirred system (though now reversed in time). Secondly, the value of u at the rear of each wave settles to the refractory branch $u \approx q$ ($= 0.0008$). This is more clearly seen in figure 4 for the smaller value of ε.

Finally, we considered the asymptotic propagation speed of these travelling waves, i.e. the speed of the front calculated after a large number of time steps. This

Table 1. *Asymptotic wave speed c_0 as calculated from the numerical solution of the unitial value problem* (6) *and* (7)

q	f	ε	c_0
0.0008	0.75	0.3	7.20
0.0008	1.0	0.3	7.02
0.0008	1.5	0.3	6.94
0.0008	0.005	0.05	40.3
0.0008	0.4	0.05	40.5
0.0008	3.0	0.05	40.7
0.008	0.4	0.05	40.5
0.08	0.4	0.05	40.5

was seen to depend very strongly on ε but only weakly on f, becoming very large as ε was decreased. Table 1 summarizes the results. One interesting feature of the asymptotic wave speed is its apparent independence of the parameter q. This point will be addressed in the next section.

5. Large time solution

Here we look for a solution of equations (6) valid for $t \gg 1$, the main features of which, as we have seen from the numerical solutions, are propagating wave fronts and, for certain parameter values, propagating wave trains. These we now concentrate on. We first introduce the travelling coordinate $y = x - s(t)$, with equation (6) then becoming

$$\frac{\partial^2 u}{\partial y^2} + \varepsilon \frac{\mathrm{d}s}{\mathrm{d}t}\frac{\partial u}{\partial y} + u(1-u) + fv\frac{(q-u)}{(q+u)} = \varepsilon \frac{\partial u}{\partial t}, \tag{33a}$$

$$\frac{\mathrm{d}s}{\mathrm{d}t}\frac{\partial v}{\partial y} + u - v = \frac{\partial v}{\partial t}, \tag{33b}$$

we look for a solution valid for $t \gg 1$ by expanding,

$$u(y,t) = u_0(y) + t^{-1}u_1(y) + \ldots, \tag{34a}$$

$$v(y,t) = v_0(y) + t^{-1}v_1(y) + \ldots, \tag{34b}$$

$$\mathrm{d}s/\mathrm{d}t = c_0 + t^{-1}c_1 + \ldots. \tag{34c}$$

At leading order we obtain the equations for the travelling front, given by

$$u_0'' + \varepsilon c_0 u_0' + u_0(1-u_0) + fv_0(q-u_0)/(q+u_0) = 0, \tag{35a}$$

$$c_0 v_0' + u_0 - v_0 = 0. \tag{35b}$$

Here primes denote differentiation with respect to the travelling coordinate y. These equations are to be solved subject to the boundary conditions

$$u_0, v_0 \to 0 \quad \text{as} \quad y \to \infty. \tag{36}$$

The conditions to be satisfied by u_0 and v_0 at the rear of the wave, i.e. as $y \to -\infty$, will be discussed below.

(a) *Wave speed selection*

The first aspect of the solution of equations (35) that we need to consider is the mechanism by which the asymptotic wave speed c_0 is selected. We note that the reaction rate in equations (35) is, for small concentrations, linear in u and v. Thus we

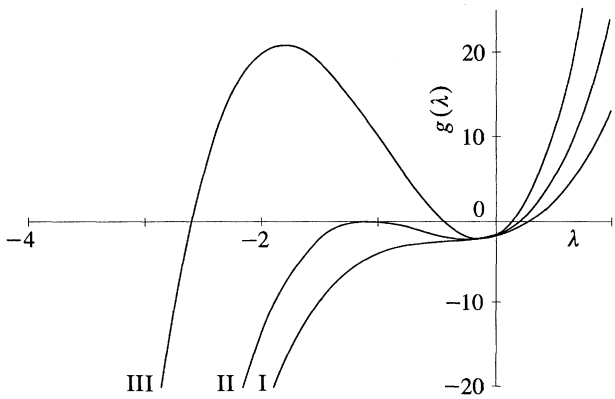

Figure 6. A graph of $g(\lambda)$ plotted against λ.

expect a structure similar to that found for the simple quadratic autocatalytic schemes discussed by Merkin & Needham (1989, 1991), and Merkin *et al.* (1989) in which the propagating front splits up into two regions. There is a region where both reaction and diffusion are important, in this y is of $O(1)$. Ahead of this is a weak diffusive region, where y is of $O(t^{\frac{1}{2}})$, and in this region the effect of diffusion is to perturb slightly the (unstable) unreacted state $u = v = 0$, hence allowing the reaction to proceed. It is then the ability of the reacting species to diffuse ahead of the wave front that controls the propagation speed of this front. We note also that this structure requires the expansion in inverse powers of t given in (34). The way in which it is the behaviour of the solution at the front of the reaction–diffusion travelling wave, in relation to the initial data, that determines the propagation speed is discussed in some detail by Billingham & Needham (1992).

We start the discussion by considering the form of u and v at the front of the reaction–diffusion wave. Here both u_0 and v_0 are small with equations (35) becoming, approximately,

$$u_0'' + \varepsilon c_0 u_0' + u_0 + f v_0 = 0, \tag{37a}$$

$$c_0 v_0' + u_0 - v_0 = 0, \tag{37b}$$

subject to boundary condition (36). On eliminating v_0 from equations (37) we obtain the third-order ordinary differential equation for u_0, given by

$$c_0 \frac{\mathrm{d}^3 u_0}{\mathrm{d}y^3} + \frac{\mathrm{d}^2 u_0}{\mathrm{d}y^2}(\varepsilon c_0^2 - 1) - c_0 \frac{\mathrm{d}u_0}{\mathrm{d}y}(\varepsilon - 1) - u_0(f+1) = 0. \tag{38}$$

On looking for a solution of equation (38) proportional to $\mathrm{e}^{\lambda y}$ we obtain the characteristic equation for λ

$$g(\lambda) \equiv c_0 \lambda^3 + (\varepsilon c_0^2 - 1)\lambda^2 + c_0(1-\varepsilon)\lambda - (1+f) = 0. \tag{39}$$

By inspection the cubic equation $g(\lambda) = 0$ has one positive root, since the coefficient of the final term is negative. The remaining two roots (if real) must be negative since $g'(0) = c_0(1-\varepsilon) > 0$, for $\varepsilon < 1$. Note that complex conjugate roots are not allowed, as this would lead to negative values of u_0 (and v_0) in violation (25). The function $g(\lambda)$ is plotted against λ for typical parameters in figure 6. The curves I, II and III correspond to the cases when the remaining two roots of $g(\lambda)$ are a complex conjugate pair, equal negative roots and two non-equal negative roots respectively. The curves I, II and III are displayed for increasing values of the parameter c_0, where I

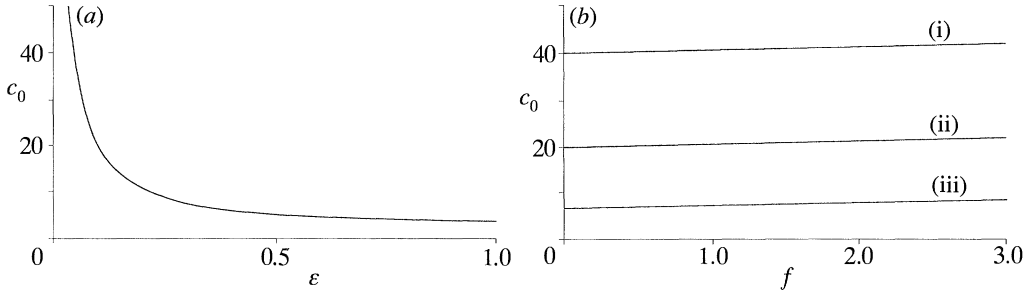

Figure 7. A graph of wave speed c_0 plotted against (*a*) ε and (*b*) f for $q = 0.0008$. (i) $\varepsilon = 0.05$, (ii) $\varepsilon = 0.1$, (iii) $\varepsilon = 0.3$.

corresponds to the smallest value of c_0 and III to the largest value. Curve II corresponds to the minimum allowable wave speed c_0^*, where $c_0 \geqslant c_0^*$ (i.e. the minimum value of c_0 which leads to a monotonically decaying solution in y). Therefore, for a minimum wave speed we require the solution of

$$g(\lambda) = 0, \quad g'(\lambda) = 0. \tag{40}$$

Now, to match with the weak diffusive region ahead of this reaction–diffusion region, we must choose the solution of equation (39) which corresponds to this minimum wave speed, i.e. we must take $c_0 = c_0^*$. This is in line with previous work on systems governed, in chemical terms, by quadratic autocatalysis, leading to the much-studied Fisher–Kolmogorov equation (Fisher 1937; Kolmogorov *et al.* 1937). For this problem there is a continuous spectrum of allowable wave speeds, as ascertained from the reaction–diffusion front equations. However, the solution of the full initial-value problem shows that the ensuing travelling wave propagates with the minimum of these allowable speeds, (see, for example, Bramson 1983). It should be pointed out though that this conclusion applies only when the initial data has compact support, travelling waves with speeds greater than this minimum are found for initial data which is more 'spread out' (Gazdag & Canosa 1974; Larson 1978).

The condition $g'(\lambda) = 0$ gives a quadratic equation in λ

$$3c_0\lambda^2 + 2(\varepsilon c_0^2 - 1)\lambda + c_0(1-\varepsilon) = 0. \tag{41}$$

Equations (39) and (41) taken together form a pair of equations which enable the minimum wave speed $c_0 = c_0^*$ and the negative eigenvalue $\lambda = -\lambda_1$ $(\lambda_1 > 0)$, corresponding to the equal roots case, to be found. Now on eliminating λ from equations (39) and (41) we obtain a cubic polynomial in c_0^2, namely

$$\varepsilon^2((1+\varepsilon)^2 + 4\varepsilon f)\, c_0^6 - (6\varepsilon(3-\varepsilon)(1+f) + 2(1-\varepsilon)^2(2-\varepsilon))\, c_0^4 + (6(1+f)(3-\varepsilon) - 27(1+f)^2 + (1-\varepsilon)^2)\, c_0^2 - 4(1+f) = 0. \tag{42}$$

Note that this cubic and hence the minimum wave speed c_0^* is independent of the parameter q. This was borne out by the numerical solutions described in the previous section.

It is not possible to proceed further analytically, for general values of the parameters for which equation (42) has to be solved numerically. Figure 7*a*, *b* shows the minimum wave speed (as found from (42)) plotted against ε (for $f = 1$) and f (for $\varepsilon = 0.05$, 0.1 and 0.3) respectively. These figures show the strong dependence of c_0 on ε, with c_0 becoming large as $\varepsilon \to 0$, and the very weak dependence of c_0 on f (for a given value ε there is only a 3.2% change in c_0 from $f = 0$ to $f = 3$). However, we can obtain asymptotic values of c_0 for small ε and for small and large f.

PHILOSOPHICAL TRANSACTIONS OF THE ROYAL SOCIETY A MATHEMATICAL, PHYSICAL & ENGINEERING SCIENCES

For $\varepsilon \ll 1$, a consideration of equation (42) shows that c_0 is of $O(\varepsilon^{-1})$, and after a little calculation we find that

$$c_0 = (1/\varepsilon)\,(2+\tfrac{1}{2}\varepsilon f+\varepsilon^2(\tfrac{3}{4}f-\tfrac{1}{2}f^2)+\ldots) \tag{43a}$$

as $\varepsilon \to 0$. The values of c_0 given by (43*a*) are in excellent agreement with those obtained numerically from equation (42), and shown in figure 7*a*, for $f = 1$. The expansion (43*a*) being only about 20% out even at $\varepsilon = 1$. The corresponding values of λ_1 are given by

$$\lambda_1 = 1+\tfrac{1}{2}f\varepsilon+\ldots. \tag{43b}$$

For $f = 0$, equation (42) can be solved exactly to give $c_0 = 2/\varepsilon$, with $\lambda_1 = 1$. Then, on expanding for small f, we find that

$$c_0 = \frac{2}{\varepsilon}+\frac{1}{(2+\varepsilon)}f+\ldots, \tag{44a}$$

$$\lambda_1 = 1+\frac{\varepsilon(4+\varepsilon)}{2(2+\varepsilon)^2}f+\ldots \tag{44b}$$

as $f \to 0$. Note that the leading order terms for small ε and for small f are the same and this explains the very weak dependence of c_0 on f as seen in figure 7*b*.

For $f \gg 1$ and ε of $O(1)$, equation (42) suggests that c_0 is of $O(f^{\frac{1}{4}})$, with further calculation giving

$$c_0 \sim (27/4\varepsilon)^{\frac{1}{4}}f^{\frac{1}{4}}+\ldots, \quad \lambda_1 \sim (4\varepsilon^3/3)^{\frac{1}{4}}f^{\frac{1}{4}}+\ldots$$

as $f \to \infty$.

We now return to the solution of equation (38), where we now have c_0 and λ determined by (39) and (41), that

$$u_0 \sim (A_0\,y+B_0)\,\mathrm{e}^{-\lambda_1 y}+\ldots \tag{46a}$$

as $y \to \infty$, for constants A_0 and B_0. The corresponding behaviour of v_0 is obtained using equation (37*b*) and is given by

$$v_0 \sim \left[\frac{A_0}{(1+\lambda_1 c_0)}y+\frac{c_0 A_0+(1+\lambda_1 c_0)B_0}{(1+\lambda_1 c_0)^2}\right]\mathrm{e}^{-\lambda_1 y}+\ldots. \tag{46b}$$

The equations at $O(t^{-1})$ are

$$u_1''+\varepsilon c_0\,u_1'+(1-2u_0)\,u_1+f\left(\frac{q-u_0}{q+u_0}\right)v_1-\frac{2fqv_0}{(q+u_0)^2}u_1 = -\varepsilon c_1\,u_0', \tag{47a}$$

$$c_0\,v_1'+u_1-v_1 = -c_1\,v_0', \tag{47b}$$

subject to

$$u_1 \to 0, \quad v_1 \to 0 \quad \text{as} \quad y \to \infty. \tag{47c}$$

From equations (47) we require the behaviour of u_1 and v_1 as $y \to \infty$. We find, after a little calculation, that

$$u_1 \sim \left[\frac{\lambda_1 c_1 A_0(f+(1+\lambda_1 c_0)^2\varepsilon)}{6((1+\lambda_1 c_0)^2+c_0^2 f/(1+\lambda_1 c_0))}y^3+\ldots\right]\mathrm{e}^{-\lambda_1 y}+\ldots, \tag{48a}$$

$$v_1 \sim \left[\frac{\lambda_1 c_1 A_0(f+(1+\lambda_1 c_0)^2\varepsilon)}{6(1+\lambda_1 c_0)\,((1+\lambda_1 c_0)^2+c_0^2 f/(1+\lambda_1 c_0))}y^3+\ldots\right]\mathrm{e}^{-\lambda_1 y}+\ldots. \tag{48b}$$

From (46) and (48) we then have, as $y \to \infty$,

$$u \sim \left\{(A_0 y + B_0) + t^{-1}\left[\frac{\lambda_1 c_1 A_0 (f + (1+\lambda_1 c_0)^2 \varepsilon)}{6((1+\lambda_1 c_0)^2 + c_0^2 f/(1+\lambda_1 c_0))} y^3 + \ldots\right]\right\} \mathrm{e}^{-\lambda_1 y} + \ldots, \tag{49}$$

together with a similar form for v. Equation (49) shows that there is a weak non-uniformity developing in this expansion when y is of $O(t^{\frac{1}{2}})$, with the term of $O(t^{-1})$ in the expansion then becoming comparable with the leading order term (though both are exponentially small). This suggests that there will be a region ahead of the reaction–diffusion front in which diffusion plays the dominant role and which is to be matched to the solution given by (49) for y large. In this region, we transform equations (33) by writing

$$u = \mathrm{e}^{-\lambda_1 y} t^{\frac{1}{2}} F(\eta, t), \quad v = \mathrm{e}^{-\lambda_1 y} t^{\frac{1}{2}} G(\eta, t), \quad \eta = y/t^{\frac{1}{2}}, \tag{50}$$

where η is now of $O(1)$. The equations satisfied by the functions F and G are

$$t^{-1}\frac{\partial^2 F}{\partial \eta^2} + t^{-\frac{1}{2}}\left[\varepsilon \frac{\mathrm{d}s}{\mathrm{d}t} - 2\lambda_1\right]\frac{\partial F}{\partial \eta} + \left[\left(\lambda_1^2 - \varepsilon\lambda_1 \frac{\mathrm{d}s}{\mathrm{d}t} + 1\right)F + fG\right] = t^{-1}\left[\tfrac{1}{2}F - \tfrac{1}{2}\eta\frac{\partial F}{\partial \eta} + t\frac{\partial F}{\partial t}\right], \tag{51a}$$

$$t^{-\frac{1}{2}}\frac{\mathrm{d}s}{\mathrm{d}t}\frac{\partial G}{\partial \eta} + \left[F - \left(1 + \lambda_1 \frac{\mathrm{d}s}{\mathrm{d}t}\right)G\right] = t^{-1}\left[\tfrac{1}{2}G - \tfrac{1}{2}\eta\frac{\partial G}{\partial \eta} + t\frac{\partial G}{\partial t}\right], \tag{51b}$$

where terms of $O(\mathrm{e}^{-\lambda_1 y})$ have been neglected in equations (51). To solve equations (51) we expand $F(\eta, t)$ and $G(\eta, t)$ in powers of $t^{-\frac{1}{2}}$, namely

$$F(\eta, t) = F_0(\eta) + t^{-\frac{1}{2}} F_1(\eta) + \ldots, \tag{52a}$$

$$G(\eta, t) = G_0(\eta) + t^{-\frac{1}{2}} G_1(\eta) + \ldots, \tag{52b}$$

with $\mathrm{d}s/\mathrm{d}t$ expanded via (34c).

At leading order we find that F_0 and G_0 satisfy the equations

$$(\lambda_1^2 - \varepsilon\lambda_1 c_0 + 1) F_0 + f G_0 = 0, \tag{53a}$$

$$F_0 - (1 + \lambda_1 c_0) G_0 = 0. \tag{53b}$$

Since λ_1 is given by the cubic equation (39), it follows that

$$(\lambda_1^2 - \varepsilon\lambda_1 c_0 + 1)(1 + \lambda_1 c_0) + f = 0 \tag{54a}$$

and hence equations (53) are satisfied for any choice of F_0, with G_0 given by

$$G_0 = F_0/(1 + \lambda_1 c_0). \tag{54b}$$

At $O(t^{-\frac{1}{2}})$ we obtain the equations

$$(\lambda_1^2 - \varepsilon c_0 \lambda_1 + 1) F_1 + f G_1 = (2\lambda_1 - \varepsilon c_0) F_0', \tag{55a}$$

$$F_1 - (1 + \lambda_1 c_0) G_1 = \frac{c_0}{1 + \lambda_1 c_0} G_0', \tag{55b}$$

where primes now denote differentiation with respect to η. Now the left-hand sides of equations (55) are the same as (53) and hence the right-hand sides must satisfy a compatibility requirement. This gives, on using (54b),

$$[(2\lambda_1 - \varepsilon c_0)(1 + \lambda_1 c_0)^2 - c_0 f] F_0' = 0. \tag{56a}$$

Using (54a), this equation becomes

$$[3c_0 \lambda_1^2 - 2(\varepsilon c_0^2 - 1)\lambda_1^2 + c_0(1 - \varepsilon)] F_0' = 0, \tag{56b}$$

which is again satisfied for any choice of F_0', since λ_1 satisfies the equal roots condition (41).

At $O(t^{-1})$ we obtain the equations

$$(\lambda_1^2-\varepsilon\lambda_1 c_0+1)F_2+fG_2 = (\varepsilon c_1\lambda_1-\tfrac{1}{2})F_0-\tfrac{1}{2}\eta F_0'-F_0''+(2\lambda_1-\varepsilon c_0)F_1', \tag{57a}$$

$$F_2-(1+\lambda_1 c_0)G_2 = (\lambda_1 c_1-\tfrac{1}{2})G_0-\tfrac{1}{2}\eta G_0'-c_0 G_1'. \tag{57b}$$

Equations (57) give a solvability condition, which, in turn, leads to an equation for $F_0(\eta)$, on using (54a) and (56b). We find that F_0 satisfies the equation

$$F_0''+\tfrac{1}{2}a\eta F_0'-bF_0 = 0, \tag{58a}$$

where

$$a = \frac{(1+\lambda_1 c_0)((1+\lambda_1 c_0)+f)^2}{(1+\lambda_1 c_0)^3+c_0^2 f},$$

which is positive and

$$b = \frac{(1+\lambda_1 c_0)[(\frac{1}{2}+\varepsilon\lambda_1 c_1)(1+\lambda_1 c_0)^2+f(\frac{1}{2}+\lambda_1 c_1)]}{(1+\lambda_1 c_0)^3+c_0^2 f}.$$

Equation (58a) has to be solved subject to

$$F_0\to 0 \quad \text{as} \quad \eta\to\infty \tag{58b}$$

and, on matching with the solution for $y \gg 1$, that

$$F_0 \sim A_0\left[\eta+\frac{\lambda_1 c_1 A_0(f+(1+\lambda_1 c_0)^2\varepsilon)}{6[(1+\lambda_1 c_0)^2+c_0^2 f/(1+\lambda_1 c_0)]}\eta^3+\ldots\right] \tag{58c}$$

as $\eta\to\infty$.

Equation (58a) has a solution satisfying (58c) in terms of confluent hypergeometric functions (Slater 1960) as

$$F_0 = A_0\,\eta\,\mathrm{e}_1^{-a\eta^2/4}F_1(1+b/a;\tfrac{3}{2};\tfrac{1}{4}a\eta^2). \tag{59a}$$

This solution does not satisfy condition (58b) unless the series given by the confluent hypergeometric function in (59a) terminates. It does so when $1+b/a = 0$ or a negative integer. However, in the latter case, the resulting polynomial in η^2 has zeros at finite values of η and consequently gives a range of η over which F_0 is negative, violating the condition that $u(x,t) \geqslant 0$ for $x \geqslant 0$, $t \geqslant 0$. Thus we must have $a+b = 0$, and, on re-arranging we obtain

$$c_1 = -\frac{3}{2\lambda_1}\frac{(f+(1+\lambda_1 c_0)^2)}{(f+\varepsilon(1+\lambda_1 c_0)^2)}, \tag{59b}$$

$$F_0 = A_0\,\eta\,\mathrm{e}^{-a\eta^2/4}. \tag{59c}$$

Note that (59b) reduces to the value for the Fisher–Kolmogorov wave when $f = 0$ (Branson 1983).

This completes the discussion of the asymptotic wave speed and we now consider the structure of the travelling wave.

(*b*) *Travelling wave structure*

Having ascertained the asymptotic wave speed c_0 in the way described above, we can return to the solution of equations (35) for the permanent form travelling wave solution of equation (6). However, to complete this discussion we need the boundary

condition to be satisfied at the rear of the wave, i.e. as $y \to -\infty$. To examine this we put

$$u_0 = u_s + U, \quad v_0 = u_s + V \tag{60}$$

and substitute into equations (35). On retaining only the leading order terms for U and V small, we obtain, after eliminating V, the equation for U

$$c_0 \frac{\mathrm{d}^3 U}{\mathrm{d}y^3} + (\varepsilon c_0^2 - 1)\frac{\mathrm{d}^2 U}{\mathrm{d}y^2} + c_0 Tr \frac{\mathrm{d}U}{\mathrm{d}y} + \Delta u = 0, \tag{61a}$$

where

$$Tr = -\varepsilon - (2fqu_s/(q+u_s)^2) + (1-2u_s)$$

and

$$\Delta = \frac{2fqu_s}{(q+u_s)^2} - \frac{f(q-u_s)}{(q+u_s)} - (1-2u_s)$$

are the trace and determinant respectively of the jacobian of the well-stirred system evaluated at the stationary state (9b). On looking for a solution of this ordinary differential equation proportional to $\mathrm{e}^{\mu y}(\mu > 0)$, we obtain the characteristic equation

$$G(\mu) \equiv c_0 \mu^3 + (\varepsilon c_0^2 - 1)\mu^2 + c_0 Tr\, \mu + \Delta = 0 \tag{61b}$$

From our knowledge of the well-stirred system, $\Delta > 0$ for all parameter values, while Tr changes sign (from negative to positive) as the stationary state (9b) changes stability (form stable to unstable) at the points of Hopf bifurcation. Note also, from the wave speed selection as given by equations (39) and (41), we must have $\varepsilon c_0^2 > 1$.

Now consider the solution of equation (61b). Since $\Delta > 0$ this equation will always have one (physically unacceptable) real negative root $\mu = -\mu_0$ (say), $\mu_0 > 0$. Moreover, if $Tr > 0$ (i.e. stationary state (9b) is temporally unstable) all the coefficients are positive and there can be no real positive roots to equation (61b). Hence a necessary condition for the existence of a positive root is that stationary state (9b) be stable (i.e. $Tr < 0$). We can show directly that at the points of Hopf bifurcation (i.e. where $Tr = 0$) $G(\mu)$ has two turning points at $\mu = 0$ (a local minimum) and at $\mu = \mu_1 = -2(\varepsilon c_0^2 - 1)/3c_0 < 0$ (a local maximum) with $G(\mu_1) > G(0) > 0$. Hence, as there can be no further turning points to this cubic, the other two roots must form a complex conjugate pair of the form $\alpha \pm \mathrm{i}\beta$ (say). A consideration of equation (61b) with $Tr = 0$ then shows that $2\alpha\mu_0 = \alpha^2 + \beta^2$. From this it follows that, when $Tr = 0$, $\alpha > 0$ and the roots have positive real part. Continuing with this, we can determine the condition under which the equation $G(\mu) = 0$ has purely imaginary roots. We find this to be given by

$$\Delta = Tr\,(\varepsilon c_0^2 - 1) \tag{62}$$

condition (62) requires $Tr > 0$. Finally, we note that when $Tr < 0$, $G(\mu)$ has two turning points at a positive (local minimum) and a negative (local maximum) value of μ. Hence, in this case the other two roots must either be both real and positive or be complex conjugates with positive real part. The above enables us to deduce that when the stationary state (9b) is temporally stable (i.e. $Tr < 0$), this solution can be approached at the rear of the wave through exponentially small terms. (Note now that focal behaviour does not violate (25) as $u_s > 0$.)

To see whether this steady state could indeed be left behind at the rear of the propagating wave we have to consider the region near the boundary where x is of $O(1)$. In this region we need the values of $u = u_0$ and $v = u_0$ (in the limit as $t \to \infty$) on

the boundary to adjust, on an $O(1)$ length scale, to steady state $u = v = u_s$. If this is the case the behaviour of the solution is determined and is that shown in figure 3*a*, *b*, *e*. In this boundary region

$$u = \bar{u}(x), \quad v = \bar{v}(x). \tag{63a}$$

Equation (6*b*) gives $\bar{v}(x) = \bar{u}(x)$, with equation (6*a*) then becoming

$$\bar{u}'' + \bar{u}(1-\bar{u}) + f\bar{u}(q-\bar{u})/(q+\bar{u}) = 0 \tag{63b}$$

subject to the boundary conditions that

$$\bar{u}(0) = u_0, \quad \bar{u} \to u_s \quad \text{as} \quad x \to \infty. \tag{63c}$$

Now primes denote differentiation with respect to x.

However, it is the behaviour of the solution as $x \to \infty$ that concerns us most. Here we put $\bar{u} = u_s + U$, where U is small for x large. Equation (63*b*) then gives, on retaining only the leading order terms, the linear equation

$$U'' - \Gamma U = 0, \tag{64a}$$

where $\Gamma = \gamma/(q+u_s)^2$, with

$$\gamma = (2u_s^3 + (4q+f-1)\,u_s^2 + (2q^2+2fq-2q)\,u_s - (1+f)\,q^2), \tag{64b}$$

where u_s is given by (9*b*). For exponential decay we must have $\gamma > 0$. It is cumbersome to proceed with the examination of this condition for general values of the parameters. However, we can exploit the forms for u_s for q small as given by (12). The form for $|1-f| \ll 1$ given by (13) is not needed as u_s is temporally unstable in this range. Using (12*a*) we find that, for $f < 1$,

$$\gamma = (1-f)^3 + 2(1+2f+3f^2)\,q + O(q^2) \tag{65a}$$

and using (12*b*) that, for $f > 1$,

$$\gamma = \frac{2f(f+1)}{(f-1)}q^2 + O(q^3). \tag{65b}$$

It is clear that in both cases the condition $\gamma > 0$ is satisfied and hence the (stable) steady state $u = v = u_s$ can be left behind the wave, with this boundary region having only a local effect and not altering the basic structure of the propagating reaction–diffusion wave. However, this picture is not seen for $f > 1$ with ε sufficiently small (figures 3*c*, *d*) with there then not being a steady state left behind after the front has passed. This point will be discussed further in the next section when we consider the solution of the travelling wave equations for ε small.

6. The travelling waves

Here we establish some properties of the permanent-form travelling wave solutions satisfying the equation

$$\frac{\mathrm{d}^2u}{\mathrm{d}y^2} + \varepsilon c_0 \frac{\mathrm{d}u}{\mathrm{d}y} + u(1-u) + fv\frac{(q-u)}{(q+u)} = 0, \tag{66a}$$

$$c_0 \frac{\mathrm{d}v}{\mathrm{d}y} + u - v = 0, \tag{66b}$$

where y is the travelling coordinate $y = x - c_0 t$ and c_0 the constant wave speed. Ahead of the wave we have

$$u, v \to 0 \quad \text{as} \quad y \to \infty, \tag{67a}$$

while behind the wave, if stationary state (9b) is stable,

$$u, v \to u_s \quad \text{as} \quad y \to \infty, \tag{67b}$$

where u_s is given by (9b). We limit our attention to the case $q < 1$.

In particular, we derive the asymptotic structure of these waves when $f \ll 1$, $f \gg 1$ and when $\varepsilon \ll 1$. However, we start by deriving a general result.

Proposition. *A permanent form travelling wave* $u(y)$, $v(y)$ *satisfies* $0 \leqslant u(y) \leqslant 1$ *and* $0 \leqslant v(y) \leqslant 1$ *on* $-\infty < y < \infty$.

Proof. From the results on the invariant set, $u(x,t) \geqslant 0$, $v(x,t) \geqslant 0$ for $-\infty < x < \infty$, $t \geqslant 0$, and so we must have

$$u(y) \geqslant 0, \quad v(y) \geqslant 0. \tag{68}$$

Hence we need to show that $u(y) \leqslant 1$ and $v(y) \leqslant 1$ on $-\infty < y < \infty$ for $q < 1$. It is straightforward to show that $u_s \leqslant 1$ for $q < 1$ for all $f \geqslant 0$. Now suppose that there is at least one range of values of y for which $u(y) > 1$. Then there will be at least one value y_1 (say) on this range at which $u(y)$ will have a local maximum, with

$$u(y_1) > 1, \quad u'(y_1) = 0, \quad u''(y_1) \leqslant 0. \tag{69a}$$

Now from equation (66a) we obtain

$$u''(y_1) = u(y_1)\,(u(y_1) - 1) + fv(y_1)\left(\frac{u(y_1) - q}{u(y_1) + q}\right) > 0. \tag{69b}$$

This gives a contradiction and hence we must have

$$0 \leqslant u(y) \leqslant 1 \quad \text{on} \quad -\infty < y < \infty. \tag{69c}$$

For $v(y)$, suppose again that $v(y) > 1$ for some range of y, then there will be a value of y, y_2 (say) at which $v(y)$ will have a local maximum with

$$v(y_2) > 1, \quad v'(y_2) = 0, \quad v''(y_2) \leqslant 0. \tag{70a}$$

However, from equation (66b),

$$c_0 v'(y_2) = 0 = v(y_2) - u(y_2), \tag{70b}$$

which in turn implies that $u(y_2) > 1$. This again leads to a contradiction. Hence we must have

$$0 \leqslant v(y) \leqslant 1 \quad \text{on} \quad -\infty < y < \infty. \tag{70c}$$

Note that this last result can be obtained directly from equation (66b), which when integrated subject to boundary conditions (67), gives

$$v(y) = \frac{\mathrm{e}^{y/c_0}}{c_0} \int_y^\infty u(s)\, \mathrm{e}^{-s/c_0}\, \mathrm{d}s \tag{71}$$

Then, for any bound on $u(y)$, say $u(y) \leqslant M$, $-\infty < y < \infty$, we have via (71) that $v(y) \leqslant M$, $-\infty < y < \infty$.

(*a*) *The structure of the travelling waves for* $f \ll 1$

We look for a solution of equations (66) valid for small f, by expanding

$$u(y;f) = u_0(y) + f u_1(y) + \ldots, \tag{72a}$$

$$v(y;f) = v_0(y) + f v_1(y) + \ldots \tag{72b}$$

and using the asymptotic expansions for the wave speed c_0 and stationary state u_s for small f derived previously, namely

$$c_0 = \frac{2}{\varepsilon} + \frac{1}{(2+\varepsilon)} f + \ldots, \tag{73a}$$

$$u_s = 1 + \frac{(q-1)}{(q+1)} f + \ldots. \tag{73b}$$

At leading order we obtain the equations

$$u_0'' + 2u_0' + u_0(1-u_0) = 0, \tag{74a}$$

$$v_0' + \tfrac{1}{2}\varepsilon(u_0 - v_0) = 0 \tag{74b}$$

(primes denoting differentiation with respect to the travelling coordinate y). Equation (74*a*) is the well known Fisher–Kolmogorov equation corresponding to the minimum wave speed. It has a solution, with the properties that

$$u_0(y) \sim \begin{cases} (y + A_0)\,\mathrm{e}^{-y} + \ldots & \text{as} \quad y \to \infty, \qquad (75a) \\ 1 - B_0\,\mathrm{e}^{\mu y} + \ldots & \text{as} \quad y \to -\infty, \qquad (75b) \end{cases}$$

where A_0 and B_0 are constants and $\mu = \sqrt{2} - 1$. Equation (74*b*) yields the solution

$$v_0(y) = \tfrac{1}{2}\varepsilon\,\mathrm{e}^{\frac{1}{2}\varepsilon y} \int_y^\infty \mathrm{e}^{-\frac{1}{2}\varepsilon s}\, u_0(s)\,\mathrm{d}s. \tag{76}$$

On considering this solution as $|y| \to \infty$ and using (75), we find that

$$v_0(y) \to \begin{cases} 0 & \text{as} \quad y \to \infty, \\ 1 & \text{as} \quad y \to -\infty. \end{cases} \tag{77}$$

Hence the solution of equations (74) satisfies all the required boundary conditions as $|y| \to \infty$, to leading order.

At $O(f)$ we obtain the linear equations

$$u_1'' + 2u_1' + (1-2u_0)\,u_1 = -\frac{\varepsilon}{(2+\varepsilon)} u_0' - v_0 \frac{(q-u_0)}{(q+u_0)}, \tag{78a}$$

$$v_1' + \tfrac{1}{2}\varepsilon(u_1 - v_1) = -\frac{\varepsilon}{2(2+\varepsilon)} v_0' \tag{78b}$$

to be solved subject to the boundary conditions that

$$\begin{aligned} u_1, v_1 &\to -\left(\frac{1-q}{1+q}\right) && \text{as} \quad y \to -\infty, \\ u_1, v_1 &\to 0 && \text{as} \quad y \to \infty. \end{aligned} \tag{79a}$$

A solution of equations (78) can be obtained which is compatible with both boundary conditions (79) and hence the expansion (72) is regular (at least to this order). Hence, for small f, the solution is a regular perturbation to the fisher–Kolmogorov solution. At the rear of the wave both u and v tend to their stable stationary states, i.e. $u, v \sim 1-((1-q)/(1+q))f+\ldots$.

(b) *The structure of the travelling waves for $f \gg 1$*

Here we use the asymptotic expansions for the wave speed c_0 and the stationary state u_s for large f, namely

$$c_0 = (27/4\varepsilon)^{\frac{1}{4}} f^{\frac{1}{4}} + \ldots, \tag{80a}$$

$$u_s = q + (1/f)\,2q(1-q) + \ldots. \tag{80b}$$

If we look for a solution of equations (66) for $f \gg 1$ by expanding in the form

$$u(y;f) = u_0(y) + \frac{1}{f} u_1(y) + \ldots, \tag{81a}$$

$$v(y;f) = v_0(y) + \frac{1}{f} v_1(y) + \ldots. \tag{81b}$$

Substituting into equations (66) and equating terms in like powers of f gives simply

$$u_0 = v_0 = q, \quad u_1 = v_1 = 2q(1-q), \tag{81c}$$

which is just expansion (80b) for u_s. Hence the solution for $f \gg 1$ must be a singular perturbation problem. Further consideration shows that the solution divides up into two regions. There is a thick outer region, of thickness of $O(f^{\frac{1}{4}})$, at the rear of the wave and a thinner inner region, of thickness of $O(f^{-\frac{1}{4}})$, at the front of the wave.

We consider first the outer region ($y < 0$) in which u and v are left unscaled, while y is rescaled by

$$Y = f^{-\frac{1}{4}} y. \tag{82}$$

At leading order we obtain the equations

$$(27/4\varepsilon)^{\frac{1}{4}} \frac{\mathrm{d}v_0}{\mathrm{d}Y} + u_0 - v_0 = 0, \tag{83a}$$

$$v_0(q-u_0)/(q+u_0) = 0 \tag{83b}$$

which yield the solutions

$$u_0 = q, \quad v_0 = q + C_0 \exp\left[(4\varepsilon/27)^{\frac{1}{4}} Y\right], \tag{84}$$

where C_0 is a constant which will be determined by the matching. Note that as $Y \to -\infty$ the boundary conditions u_0, $v_0 \to u_s$ is satisfied to leading order.

At $O(f^{-1})$ we obtain the equations

$$u_0(1-u_0) - v_0 u_1/2q = 0, \tag{85a}$$

$$(27/4\varepsilon)^{\frac{1}{4}} \frac{\mathrm{d}v_1}{\mathrm{d}Y} + u_1 - v_1 = 0, \tag{85b}$$

with solutions

$$u_1 = \frac{2q(1-q)}{1+(C_0/q)\exp\left[(4\varepsilon/27)^{\frac{1}{4}} Y\right]}, \tag{86a}$$

$$v_1 = 2q(1-q) + \exp\left[(4\varepsilon/27)^{\frac{1}{4}} Y\right]\left[B_0 + 2C_0(1-q)\log\left(\frac{\exp\left[(4\varepsilon/27)^{\frac{1}{4}} Y\right]}{1+(C_0/q)\exp\left[(4\varepsilon/27)^{\frac{1}{4}} Y\right]}\right)\right], \tag{86b}$$

where B_0 is a further constant. Again the boundary conditions as $Y \to \infty$ are satisfied by (86).

The boundary conditions $(u, v \to 0)$ at the front of the wave are not satisfied and a further inner region is required in which this is achieved. In this region (of thickness $O(f^{-\frac{1}{4}})$) we rescale variables by writing

$$u = U, \quad v = f^{-\frac{1}{2}} V, \quad \bar{y} = f^{\frac{1}{4}} y, \tag{87}$$

where U, V and $\bar{y}$ are all of $O(1)$ in this region.

At leading order we obtain the equations

$$(27/4\varepsilon)^{\frac{1}{4}} \frac{\mathrm{d}V}{\mathrm{d}\bar{y}} + U = 0, \tag{88a}$$

$$\frac{\mathrm{d}^2 U}{\mathrm{d}\bar{y}^2} + \varepsilon (27/4\varepsilon)^{\frac{1}{4}} \frac{\mathrm{d}U}{\mathrm{d}\bar{y}} + V \frac{(q-U)}{(q+U)} = 0 \tag{88b}$$

to be solved subject to

$$U \to 0, \quad V \to 0 \quad \text{as} \quad \bar{y} \to \infty. \tag{88c}$$

Now the solution in this region as $\bar{y} \to -\infty$ has to match with the solution in the outer region as $Y \to 0$. From (84) we have $v \sim C_0 + q + \ldots$ as $Y \to 0$, which is of $O(1)$ and thus will not match with v in the inner region (where v is of $O(f^{-\frac{1}{2}})$) unless we take

$$C_0 = -q.$$

This determines the constant C_0 and with this we then have from (84) and (86) that

$$U \sim q - [2(27/4\varepsilon)^{\frac{1}{4}} q(1-q)\, \bar{y}^{-1}] f^{-\frac{1}{2}} + \ldots, \tag{90a}$$

$$V \sim -q(4\varepsilon/27)^{\frac{1}{4}} \bar{y} + \ldots \tag{90b}$$

as $\bar{y} \to -\infty$.

Equation (88a) can be integrated to give

$$V(\bar{y}) = (4\varepsilon/27)^{\frac{1}{4}} \int_{\bar{y}}^{\infty} U(s)\, \mathrm{d}s. \tag{91}$$

The solution in this inner region then requires the solution of equation (88b) subject to boundary conditions (88c) and (90). We are unable to proceed any further analytically, but the structure of the reaction–diffusion travelling wave for f large is now clear. There is an outer region of thickness $O(f^{\frac{1}{4}})$ in which u remains constant to leading order and in which v starts by being of $O(1)$ at the rear becoming smaller, of $O(f^{-\frac{1}{2}})$ at the front. There is then a much thinner inner region, of thickness $O(f^{-\frac{1}{4}})$, in which u is of $O(1)$ and v is small of $O(f^{-\frac{1}{2}})$, and in which the conditions ahead of the wave are attained.

(*c*) *The structure of the travelling wave for* $\varepsilon \ll 1$

Finally, we look for a solution of equation (66) valid for $\varepsilon \ll 1$. We start by expanding

$$u(y;\varepsilon) = u_0(y) + \varepsilon u_1(y) + \ldots, \tag{92a}$$

$$v(y;\varepsilon) = v_0(y) + \varepsilon v_1(y) + \ldots, \tag{92b}$$

and using the asymptotic expansion for the wave speed c_0 for small ε, namely

$$c_0 = (2/\varepsilon) + \tfrac{1}{2}f + O(\varepsilon). \tag{92c}$$

Note that stationary state (9b) does not depend on ε.

At leading order we obtain the equations

$$u_0'' + 2u_0' + u_0(1-u_0) + fv_0\frac{(q-u_0)}{(q+u_0)} = 0, \tag{93a}$$

$$v_0' = 0. \tag{93b}$$

Equation (93b) together with the boundary conditions at the front of the wave gives $v_0 = 0$, with equation (93a) then becoming the equation for the Fisher–Kolmogorov wave with minimum speed. The behaviour of the solution of equation (93a) as $|y| \to \infty$ is given by (75). Note that the boundary conditions $u_0 \to 0$, $v_0 \to 0$ as $y \to \infty$ are satisfied. Also $u_0 \to 1$ as $y \to -\infty$ and the boundary conditions at the rear of the wave are not satisfied. Hence we have a singular perturbation problem and to obtain more information about the non-uniformity in expansions (92a, b) we need to consider the equations for the terms of $O(\varepsilon)$.

At $O(\varepsilon)$, we obtain the equations

$$u_1'' + 2u_1' + (1-2u_0)\,u_1 + f\frac{(q-u_0)}{(q+u_0)}v_1 = -\tfrac{1}{2}fu_0', \tag{94a}$$

$$2v_1' + u_0 = 0. \tag{94b}$$

Equation (94b) has the solution

$$v_1 = \frac{1}{2}\int_y^\infty u_0(s)\,\mathrm{d}s, \tag{94c}$$

which gives $v_1 \to 0$ as $y \to \infty$ (satisfying the boundary condition at the wave front) and has $v_1 \sim -\frac{1}{2}y + \ldots$ as $y \to -\infty$. On considering equation (94a) as $y \to \infty$, we note that $u_1 \to 0$ again satisfying the boundary condition at the front of the wave. However, as $y \to -\infty$ equation (94a) gives

$$u_1 \sim \frac{f(1-q)}{2(1+q)}y + \ldots. \tag{94d}$$

Hence expansion (92a) becomes non-uniform as $y \to -\infty$ when $\varepsilon|y|$ is of $O(1)$, i.e. when $|y|$ is of $O(\varepsilon^{-1}) \gg 1$ with then both u and v being of $O(1)$.

This suggests that we need a further region, of thickness $O(\varepsilon^{-1})$, at the rear of the wave in which we introduce the stretched variable $\bar{Y} = \varepsilon y$ ($\bar{Y} < 0$) and leave u and v unscaled. Equations (66) become

$$\varepsilon^2\frac{\mathrm{d}^2u}{\mathrm{d}\bar{Y}^2} + \varepsilon^2 c_0\frac{\mathrm{d}u}{\mathrm{d}\bar{Y}} + u(1-u) + fv\frac{(q-u)}{(q+u)} = 0, \tag{95a}$$

$$\varepsilon c_0\frac{\mathrm{d}v}{\mathrm{d}\bar{Y}} + u - v = 0. \tag{95b}$$

PHILOSOPHICAL TRANSACTIONS OF THE ROYAL SOCIETY A MATHEMATICAL, PHYSICAL & ENGINEERING SCIENCES

With again c_0 expanded for small ε via (92c). The leading order terms (u_0, v_0) in an expansion in powers of ε then satisfy the equations

$$2\frac{\mathrm{d}v_0}{\mathrm{d}\bar{Y}} + u_0 - v_0 = 0, \tag{96a}$$

$$u_0(1-u_0) + fv_0\frac{(q-u_0)}{(q+u_0)} = 0. \tag{96b}$$

Equations (96) are to be solved subject to the boundary conditions that

$$u_0, v_0 \to u_s \quad \text{as} \quad \bar{Y} \to -\infty, \tag{97a}$$

and, on matching with the inner solution, that

$$u_0 \sim 1 + \tfrac{1}{2}f\frac{(1-q)}{(1+q)}\bar{Y} + \ldots, \tag{97b}$$

$$v_0 \sim -\tfrac{1}{2}\bar{Y} + \ldots \tag{97c}$$

as $\bar{Y} \to O^-$.

On rearranging equation (96b) we obtain

$$\frac{\mathrm{d}u_0}{\mathrm{d}\bar{Y}} = \frac{1}{2}\frac{u_0(u_0-q)(u_0-u_s)(u_0+\bar{u}_s)}{(2u_0^3-(1+2q)u_0^2+2q(1-q)u_0+q^2)}, \tag{98a}$$

$$\frac{\mathrm{d}v_0}{\mathrm{d}\bar{Y}} = -\frac{1}{2}\frac{u_0(u_0-u_s)(u_0+\bar{u}_s)}{f(u_0-q)}, \tag{98b}$$

where $\bar{u}_s = \frac{1}{2}(\sqrt{[(f+q-1)^2+4q(1+f)]}-1+f+q) > 0$. It is straightforward to show that $1 > u_s > q$ for $f > 0$. Then, since (98a) gives

$$\frac{\mathrm{d}u_0}{\mathrm{d}\bar{Y}} = \frac{(1-u_s)(1+\bar{u}_s)}{2(1+q)} > 0$$

at $u_0 = 1$, a monotone increasing solution of equation (98a) can be determined which satisfies the boundary conditions (97) (with a corresponding monotone decreasing solution of equation (98b) being found), provided the denominator in equation (98a) is non-zero over the range $u_s \leqslant u_0 \leqslant 1$.

Hence we need to consider the function

$$D = 2u^3-(1+2q)u^2+2q(1-q)u+q^2 \tag{99}$$

over the range $u_s \leqslant u \leqslant 1$. At $u = 1$, $D = 1-q^2 > 0$. Also,

$$\mathrm{d}D/\mathrm{d}u = 2(u-q)(3u-(1-q)) \tag{100a}$$

giving turning points at

$$u_1 = q, \quad u_2 = \tfrac{1}{3}(1-q). \tag{100b}$$

First consider the case $q > \frac{1}{4}$. Here $u_1 > u_2$ and a consideration of the second derivative of D at $u = u_1$ and $u = u_2$ shows that $u_1 = q < u_s$ is a local minimum and u_2 a local maximum. Then since $D(q) = 2q^2(1-q) > 0$ it follows that in this case $D > 0$ for all u in the range $u_s \leqslant u \leqslant 1$, and the required solution to equation (98a) can be found. For $q = \frac{1}{4}$, $u_1 = u_2 = \frac{1}{4}$, $D = 2(u-\frac{1}{4})^3+\frac{3}{32} > 0$ for all u in $u_s \leqslant u \leqslant 1$ and again no problem is encountered in solving equation (98a).

Next consider the case $q < \frac{1}{4}$. Here $u_1 < u_2$ with u_1 now being a local maximum and u_2 a local minimum, with

$$D(u_2) = \tfrac{1}{27}(10q^3 + 6q^2 + 12q - 1). \tag{101}$$

Then clearly if $D(u_2) > 0$, $D(u) > 0$ for all $u > 0$ and, in particular, for all u on $u_s \leqslant u \leqslant 1$. If however, $D(u_2) < 0$ further considerations are necessary. The equation $D(u_2) = 0$ has to be solved numerically, giving the single positive root at $q = q_0 = 0.079\,732$ (note this is effectively the same value as q_* given in (11), the value of q above which the well-stirred system is non-oscillatory). Hence, for $q > q_0$, $D(u) > 0$ for all u in the range $u_s \leqslant u \leqslant 1$ and equation (98a) is solvable.

For $q < q_0$, $D(u_2) < 0$ and, since $D(u)$ is monotone increasing on $u_2 \leqslant u \leqslant 1$, equation (99) will have a root at $u = u_3$ (say) where $u_2 = \frac{1}{3}(1-q) < u_3 < 1$. Hence for $D(u) > 0$ on $u_s \leqslant u \leqslant 1$, we require $u_3 < u_s$ or, equivalently, $D(u_s) > 0$. Otherwise equation (99) will have a root on $u_s < u < 1$ and the problem given by equations (98) and boundary condition (97) will not have a solution. It is somewhat intractable to proceed with the condition $D(u_s) > 0$ for general values of the parameters. However, we can exploit the forms for u_s valid for small q given previously, (note that q_0 is itself a small number). Using (12a) we find that, for $f < 1$,

$$D(u_s) = (1-f)^2(1-2f) + 2f(5-7f)\,q + \ldots. \tag{102}$$

From (102), $D(u_s) > 0$ for $f < \frac{1}{2}$, to leading order, which is precisely the condition (15) that u_s is a stable stationary state. However, for $f > 1$, u_s is of $O(q)$ which will be small in relation to u_2 (at which point $D < 0$) and hence equation (99) will have zeros on $u_s \leqslant u \leqslant 1$.

We are now in a position to interpret the structure of the solution of equations (66) for $\varepsilon \ll 1$. For $q > q_0$ a solution is always possible in which there is a region of thickness $O(1)$ at the front of the wave where u is $O(1)$ and v is small, of $O(\varepsilon)$. At the rear of this region is a much thicker region, of extent of $O(\varepsilon^{-1})$, in which u and v are both of $O(1)$ and at the rear of which the uniform steady state $u = v = u_s$ is attained. This picture is the same for $q < q_0$, provided that $f < \frac{1}{2} + O(q)$, i.e. the stationary state at the rear of the wave is stable. However, for $f > 1$ there is no such structure, even when u_s is stable. This is borne out by the numerical solutions where we saw, for $f = 3.0$ and $\varepsilon = 0.05$, a series of propagating pulses initiated at the boundary (figure 3c, d).

7. Discussion

In this paper we have considered the structure and speed of constant velocity wavefront solutions for a one dimensional system with BZ kinetics. Initially, the system is assembled at an unstable steady state ($u = v = 0$). The wave is initiated and sustained by imposing a constant value for one of the reactant species X at the origin. The species Z is immobilized in the reaction zone. The kinetic parameters q, ε and f have been varied to cover a range of cases, such that the corresponding non-zero steady state of the well-stirred system may be either stable or unstable. With an unstable non-zero state, the system displays a stable limit cycle in the ordinary differential equation (ODE) case. For our reaction–diffusion problem, such parameters set up an essentially phase-wave behind the front: at any given point, the concentrations u and v follow time-periodic variations that follow closely the corresponding oscillations for the well-stirred system.

If the steady state behind the wave is sufficiently stable, the reaction–diffusion

problem evolves to this solution, with a thin transition region close to the origin to satisfy the boundary condition if $u_0 \neq u_s$. For excitable systems, however, and if the boundary condition imposes a sufficiently high concentration u_0, the stable steady state is not attained after the initial front. A supercritical disturbance is realized before u approaches u_s and a second reaction pulse is initiated. Successive repetitions lead to the establishment of a periodic spatiotemporal response even though the corresponding ODE has a stable steady state: a periodic wave train has emerged in this system with a constant imposed concentration at $x = 0$.

References

Billingham, J. & Needham, D. J. 1992 The development of travelling waves in quadratic and cubic autocatalysis with unequal diffusion rates, III. Large time development in quadratic autocatalysis. *Quart. appl. Math.* **50**, 343–372.

Bramson, M. D. 1983 Convergence of solutions of the Kolmogorov equation for travelling waves. *Mem. Am. math. Soc.* **285**.

Britton, N. F. 1986 *Reaction–diffusion equations and their applications to biology*. London: Academic Press.

Crowley, M. F. & Field, R. J. 1984 Asymptotic solutions of a reduced Oregonator model of the Belousov–Zhabotinsky reaction. *J. phys. Chem.* **88**, 762–766.

Field, R. J. & Noyes, R. M. 1973 Oscillations in chemical systems. IV. Limit cycle behaviour in a model of a real chemical reaction. *J. chem. Phys.* **60**, 1877–1884.

Field, R. J. & Troy, W. C. 1979 The existence of solitary travelling wave solutions of a model of the Belousov–Zhabotinskii reaction. *SIAM J. appl. Math.* **37**.

Fisher, R. A. 1937 The wave of advance of advantageous genes. *Ann. Eugenics* **7**, 355–369.

Gazdag, J. & Canosa, J. 1974 Numerical solution of Fisher's equation. *J. appl. Probabil.* **11**, 445–457.

Gray, P., Merkin, J. H., Needham, D. J. & Scott, S. K. 1990 The development of travelling waves in a simple isothermal chemical system. III. Cubic and mixed autocatalysis. *Proc. R. Soc. Lond.* A **430**, 509–524.

Kolmogorov, A. N., Petrovsky, I. & Piscounov, N. 1937 Etude de l'equation de la diffusion avec croissacne de la quantité de matiere et son application à un probleme biologique. *Moscow Univ. Bull. Math.* **1**, 1–25.

Larson, D. A. 1978 Transient bounds and time-asymptotic behaviour of solutions to nonlinear equations of Fisher type. *SIAM J. appl. Math.* **34**, 93–103.

Leach, J. A. 1991 Ph.D. thesis, University of Leeds, U.K.

Maselko, J., Reckley, J. C. & Showalter, K. 1989 Regular and irregular spatial Patterson in an immunobilised-catalyst Belousov–Zhabotinsky reaction. *J. phys. Chem.* **93**, 2774–2780.

Maselko, J. & Showalter, K. 1989 Chemical waves on spherical surfaces. *Nature, Lond.* **339**, 609–611.

Maselko, J. & Showalter, K. 1991 Chemical waves in inhomogeneous excitable media. *Physica* D **49**, 21–32.

Merkin, J. H. & Needham, D. J. 1989 Propagating reaction–diffusion waves in a simple isothermal quadratic autocatalytic chemical system. *J. Engng Math.* **23**, 343–356.

Merkin, J. H. & Needham, D. J. 1990 The development of travelling waves in a simple isothermal chemical system. II. Cubic autocatalysis with quadratic and linear decay. *Proc. R. Soc. Lond.* A **430**, 315–345.

Merkin, J. H. & Needham, D. J. 1991 The development of travelling waves in a simple isothermal chemical system. IV. Quadratic autocatalysis with quadratic decay. *Proc. R. Soc. Lond.* A **434**, 531–554.

Merkin, J. H., Needham, D. J. & Scott, S. K. 1989 The development of travelling waves in a simple isothermal chemical system. I. Quadratic autocatalysis with linear decay. *Proc. R. Soc. Lond.* A **435**, 187–209.

PHILOSOPHICAL TRANSACTIONS OF THE ROYAL SOCIETY A MATHEMATICAL, PHYSICAL & ENGINEERING SCIENCES

Murray, J. D. 1989 *Mathematical biology*. Berlin: Springer-Verlag.

Slater, L. J. 1960 *Confluent hypergeometric functions*. Cambridge University Press.

Tyson, J. J. 1979 Oscillations, bistability and echo waves in models of the Belousov–Zhabotinskii reaction. *Ann. New York Acad. Sci.* **316**.

Tyson, J. J. & Fife, P. C. 1980 Target patterns in a realistic model of the Belousov–Zhabotinskii reaction. *J. chem. Phys.* **73**, 2224–2237.

Tyson, J. J. & Keener, J. P. 1988 Singular perturbation theory of travelling waves in excitable media (a review). *Physica* D **32**, 327–361.

Watson, E. J. 1981 *Laplace transforms and applications*. London: Van Nostrand Reinhold.

Winston, D., Arora, M., Maselko, J., Guspar, V. & Showalter, K. 1991 Cross-membrane coupling of chemical spatiotemporal patterns. *Nature, Lond.* **351**, 132–135.

Received 31 October 1991; revised 9 October 1992; accepted 20 January 1993

PHILOSOPHICAL TRANSACTIONS OF THE ROYAL SOCIETY A MATHEMATICAL, PHYSICAL & ENGINEERING SCIENCES